NASA/TM—2001-210697

Quantifying Residual Stresses by Means of Thermoelastic Stress Analysis

Andrew L. Gyekenyesi
Ohio Aerospace Institute, Brook Park, Ohio

George Y. Baaklini
Glenn Research Center, Cleveland, Ohio

February 2001

The NASA STI Program Office . . . in Profile

Since its founding, NASA has been dedicated to the advancement of aeronautics and space science. The NASA Scientific and Technical Information (STI) Program Office plays a key part in helping NASA maintain this important role.

The NASA STI Program Office is operated by Langley Research Center, the Lead Center for NASA's scientific and technical information. The NASA STI Program Office provides access to the NASA STI Database, the largest collection of aeronautical and space science STI in the world. The Program Office is also NASA's institutional mechanism for disseminating the results of its research and development activities. These results are published by NASA in the NASA STI Report Series, which includes the following report types:

- TECHNICAL PUBLICATION. Reports of completed research or a major significant phase of research that present the results of NASA programs and include extensive data or theoretical analysis. Includes compilations of significant scientific and technical data and information deemed to be of continuing reference value. NASA's counterpart of peer-reviewed formal professional papers but has less stringent limitations on manuscript length and extent of graphic presentations.

- TECHNICAL MEMORANDUM. Scientific and technical findings that are preliminary or of specialized interest, e.g., quick release reports, working papers, and bibliographies that contain minimal annotation. Does not contain extensive analysis.

- CONTRACTOR REPORT. Scientific and technical findings by NASA-sponsored contractors and grantees.

- CONFERENCE PUBLICATION. Collected papers from scientific and technical conferences, symposia, seminars, or other meetings sponsored or cosponsored by NASA.

- SPECIAL PUBLICATION. Scientific, technical, or historical information from NASA programs, projects, and missions, often concerned with subjects having substantial public interest.

- TECHNICAL TRANSLATION. English-language translations of foreign scientific and technical material pertinent to NASA's mission.

Specialized services that complement the STI Program Office's diverse offerings include creating custom thesauri, building customized data bases, organizing and publishing research results . . . even providing videos.

For more information about the NASA STI Program Office, see the following:

- Access the NASA STI Program Home Page at ***http://www.sti.nasa.gov***

- E-mail your question via the Internet to help@sti.nasa.gov

- Fax your question to the NASA Access Help Desk at 301–621–0134

- Telephone the NASA Access Help Desk at 301–621–0390

- Write to:
  NASA Access Help Desk
  NASA Center for AeroSpace Information
  7121 Standard Drive
  Hanover, MD 21076

NASA/TM—2001-210697

Quantifying Residual Stresses by Means of Thermoelastic Stress Analysis

Andrew L. Gyekenyesi
Ohio Aerospace Institute, Brook Park, Ohio

George Y. Baaklini
Glenn Research Center, Cleveland, Ohio

Prepared for the
Nondestructive Evaluation of Aging Materials and Composites IV
sponsored by the Society of Photo-Optical Instrumentation Engineers
Newport Beach, California, March 8–9, 2000

National Aeronautics and
Space Administration

Glenn Research Center

February 2001

Trade names or manufacturers' names are used in this report for identification only. This usage does not constitute an official endorsement, either expressed or implied, by the National Aeronautics and Space Administration.

Available from

NASA Center for Aerospace Information
7121 Standard Drive
Hanover, MD 21076
Price Code: A03

National Technical Information Service
5285 Port Royal Road
Springfield, VA 22100
Price Code: A03

Available electronically at http://gltrs.grc.nasa.gov/GLTRS

Quantifying Residual Stresses by Means of Thermoelastic Stress Analysis

Andrew L. Gyekenyesi
Ohio Aerospace Institute
Brook Park, Ohio 44142

George Y. Baaklini
National Aeronautics and Space Administration
Glenn Research Center
Cleveland, Ohio 44135

ABSTRACT

This study focused on the application of the Thermoelastic Stress Analysis (TSA) technique as a tool for assessing the residual stress state of structures. TSA is based on the fact that materials experience small temperature changes when compressed or expanded. When a structure is cyclically loaded, a surface temperature profile results which correlates to the surface stresses. The cyclic surface temperature is measured with an infrared camera. Traditionally, the amplitude of a TSA signal was theoretically defined to be linearly dependent on the cyclic stress amplitude. Recent studies have established that the temperature response is also dependent on the cyclic mean stress (i.e., the static stress state of the structure). In a previous study by the authors, it was shown that mean stresses significantly influenced the TSA results for titanium and nickel based alloys.[1] This study continued the effort of accurate direct measurements of the mean stress effect by implementing various experimental modifications. In addition, a more in-depth analysis was conducted which involved analyzing the second harmonic of the temperature response. By obtaining the amplitudes of the first and second harmonics, the stress amplitude and the mean stress at a given point on a structure subjected to a cyclic load can be simultaneously obtained. The experimental results showed good agreement with the theoretical predictions for both the first and second harmonics of the temperature response. As a result, confidence was achieved concerning the ability to simultaneously obtain values for the static stress state as well as the cyclic stress amplitude of structures subjected to cyclic loads using the TSA technique. With continued research, it is now feasible to establish a protocol that would enable the monitoring of residual stresses in structures utilizing TSA.

1. INTRODUCTION

Thermoelastic stress analysis (TSA) is a full-field, non-contacting technique for surface stress mapping of structures. TSA is based on the fact that materials experience a temperature change when compressed or expanded (i.e., experience a change in volume). If the load causing the volumetric change is removed and the material returns to its original temperature and shape, the process is deemed reversible. This reversibility is achieved when a material is loaded elastically at a high enough rate so as to eliminate significant conduction of heat. The thermoelastic temperature change, in steel for instance, as a result of an applied cyclic load of 1.0 MPa (145 psi) is on the order of 0.001 °C.[2]

Lord Kelvin[3] first quantified an analytical relationship between the change in temperature and the change in stress. The formulation is as follows

$$\frac{\delta T}{T_o} = \frac{-\alpha\, \delta I_1}{\rho\, C_p} \tag{1}$$

$$= -K\, \delta I_1 \tag{2}$$

where δT is the cyclic change in temperature; α is the coefficient of linear thermal expansion; T_o is the absolute temperature of the specimen; δI_1 is the change in the sum of the principal stresses; ρ is the material density; C_p is the specific heat at constant pressure; and K is the thermoelastic constant. Note that the formulations of Equations (1) and (2) indicate that δT is

independent of the mean stress. Therefore, δT is assumed to remain constant for a given stress range, δI_1, and absolute temperature, T_o, regardless of the applied mean stress.

In recent years, experimental data as well as theoretical formulations have shown a mean stress dependence concerning the thermoelastic constant, K. Such stress dependence was illustrated experimentally by Machin et al.[4] and Dunn et al.[5] The theoretical explanation for this non-linear response was defined by Wong et al.[6] Additional experimental evidence of the mean stress effect was provided in Wong et al.[7] In Wong et al.[6], the reformulated theory shows that the mean stress dependence of the thermoelastic parameter (earlier referred to as a constant) is fully accounted for by the temperature dependence of the elastic moduli of the material.

In this paper, further experimental verification of the mean stress effect is provided. This includes both a direct measure of the TSA signal as a function of the mean stress as well as an in-depth analysis of the first and second harmonics of the TSA signal. The theory, as described in the following section, shows that the thermoelastic response of a structure subjected to a pure sinusoidal mechanical load with a frequency, ω, produces a TSA signal with frequency components at the primary frequency, ω, as well as the second harmonic, 2ω. The first harmonic of the thermal response is a function of the cyclic stress amplitude and the mean stress while the second harmonic is a function of the square of the stress amplitude. By obtaining the TSA amplitudes of the first and second harmonics, the stress amplitude and the mean stress at a given point on a structure subjected to a cyclic load can be simultaneously obtained. Furthermore, comparisons are made between the theoretical predictions and the experimental data. Once confidence is achieved concerning the measured TSA response, then steps can be taken for developing empirical relationships between the TSA signal and the cyclic stress state of various materials.

It should be noted that the past thermoelastic data (references 4 through 7) were produced utilizing TSA systems with infrared (IR) cameras based on a single detector. This single detector camera incorporates a network of scanning mirrors to provide an image of an area. In references 4 through 7, the scanning devices were disengaged and only the information from a single point on the specimens was analyzed. For this study (as well as the data produced by the authors in reference 1), the TSA system uses an IR camera with a 128 x 128 focal plane array (FPA) of detectors. As a result, the reported IR detector response is based on the average of an array of detectors representing a larger two-dimensional area on the specimen surface. To obtain the first and second harmonics of a TSA signal composed of an array of IR detectors, hardware modifications of the current TSA system were required and are detailed in the Experimental Methods section.

Because this research continued the efforts of reference 1, the same metallic alloys were utilized. These included the titanium base alloys, TIMETAL 21S and Ti-6Al-4V, as well as a nickel base alloy, Inconel 718. These materials are utilized by the aviation industry in propulsion components due to their relative lightweight, high strength and stiffness, as well as their property retention at elevated temperatures.

During manufacturing, certain components, which are subjected to a cyclic fatigue environment, are fabricated so as to contain compressive residual stresses on the surface. These compressive stresses inhibit the nucleation of cracks. As a result of overloads and elevated temperature excursions, the induced residual stresses dissipate while the component is still in service, in turn, lowering its resistance to crack initiation. Once confidence is achieved concerning reliable TSA measurements of the mean stress effect, research can focus on the application of the method to residual stress assessment. Such measurements will assist in the characterization of materials in the laboratory as well as in-situ monitoring of the current residual stress state in actual structural components during fabrication and service.

2. THEORY

The revised thermoelastic equation (derived in Wong et al.[6]) relating the rate of temperature change and the rate of change in the stress state in a homogeneous Hookean material under adiabatic conditions can be written as

$$\rho_o C_\varepsilon \frac{\dot{T}}{T} = -\left[\alpha + \left(\frac{\nu}{E^2}\frac{\partial E}{\partial T} - \frac{1}{E}\frac{\partial \nu}{\partial T}\right) I_1\right]\dot{I}_1 + \left[\frac{(1+\nu)}{E^2}\frac{\partial E}{\partial T} - \frac{1}{E}\frac{\partial \nu}{\partial T}\right]\sum_{i=1}^{3}\sigma_{ii}\dot{\sigma}_{ii} \qquad (3)$$

where T is the thermodynamic temperature (Kelvin); σ_{ii} are the principal stresses (N/m^2); I_1 is the sum of the principal stresses, (N/m^2); ρ_o is the density (kg/m^3); C_ε is the specific heat under constant strain (N m/°C kg); α is the coefficient of thermal expansion ($°C^{-1}$); E is the Young's modulus (N/m^2); and ν is the Poisson's ratio. The dotted symbols represent

derivatives with respect to time. Notice that for the reformulated thermoelastic equation, the elastic moduli are not assumed constant, but are taken as functions of temperature. Hence, the difference when comparing the new formulation to the classical thermoelastic theory of Equations (1) and (2). It is also seen that the temperature response is now dependent on both the stress rate and the stress state.

Following the procedure set forth in Wong et al.[7], the uniaxial case is taken as an example. The uniaxial case is defined as having

$$\sigma_{11} = I_1, \quad \sigma_{22} = \sigma_{33} = 0 \tag{4}$$

and

$$\dot{\sigma}_{11} = \dot{I}_1, \quad \dot{\sigma}_{22} = \dot{\sigma}_{33} = 0 \tag{5}$$

Utilizing Equations (4) and (5), Equation (3) simplifies to

$$\rho_o C_\varepsilon \frac{\dot{T}}{T} = -\left(\alpha - \frac{1}{E^2}\frac{\partial E}{\partial T}\sigma_{11}\right)\dot{\sigma}_{11} \tag{6}$$

In keeping with the approach taken by Wong et al.[7], a sinusoidal stress input of the following form is defined

$$\sigma = \sigma_m + \sigma_{amp} \sin \omega t \tag{7}$$

where σ_m and σ_{amp} are the mean and amplitude of the applied stress, respectively, and ω is the loading frequency. Note that for ease of presentation the subscripts on the stress terms have been omitted with the understanding that $\sigma = \sigma_{11}$. Next, Equation (7) is substituted into Equation (6) to obtain the following solution for the uniaxial case

$$\rho_o C_t \frac{\delta T}{T_o} = -\left(\alpha - \frac{1}{E^2}\frac{\partial E}{\partial T}\sigma_m\right)\sigma_{amp} \sin \omega t - \frac{1}{4E^2}\frac{\partial E}{\partial T}(\sigma_{amp})^2 \cos 2\omega t \tag{8}$$

Note that the thermal response of a structure subjected to a pure sinusoidal mechanical excitation produces a thermal signature function that has components at both the primary loading frequency, ω, as well as the second harmonic, 2ω. The first harmonic of the thermal response is a function of the cyclic stress amplitude and the mean stress while the second harmonic is a function of the square of the stress amplitude. It is now apparent that by obtaining the first and second harmonics, it is possible to obtain both the cyclic stress amplitude and the mean stress.

Lastly, comparing Equations (1) and (2) with Equations (6) and (8), the effective K for a homogeneous Hookean material subjected to a uniaxial stress is derived as

$$K = \left(\alpha - \frac{1}{E^2}\frac{\partial E}{\partial T}\sigma_m\right)(\rho\, C_\varepsilon)^{-1} \tag{9}$$

Equation (9) shows that the thermoelastic parameter is a linear function of the mean stress, σ_m. A normalized measure of the thermoelastic parameter's mean stress dependence can be expressed as

$$\frac{1}{K_o}\frac{\partial K}{\partial \sigma_m} = \frac{-1}{\alpha E^2}\frac{\partial E}{\partial T} \tag{10}$$

where

$$K_o = \frac{\alpha}{\rho C_\varepsilon} \tag{11}$$

Equation (10) simply gives the slope of the thermoelastic constant (in a dimensionless, normalized form) in respect to the mean stress, σ_m. Note that Equation (11) is the zero mean stress solution of Equation (9).

3. EXPERIMENTAL METHODS

Three metallic alloys with various pre-test heat treatments were analyzed for this study. Two were titanium base and one was a Nickel base. The first titanium alloy, sheet TIMETAL 21S, was heat-treat stabilized at 621 °C (1150 °F) for 8 hours. The second titanium alloy, Ti-6Al-4V in sheet form, was annealed at 788 °C (1450 °F) for 15 minutes and then air cooled. The Nickel base Inconel 718 sheet plates were solution treated at 1038 °C (1900 °F) and quick cooled. The material was then aged at 718 °C (1325 °F) for 8 hours. Next, it was cooled at a rate of 56 °C (100 °F/hour) to 621°C (1150 °F) and held for 8 hours. This was followed by a quick cool.

The TIMETAL 21S was supplied as round, reduced gage section coupons machined from 0.79 cm (0.31 in.) thick, flat plates. The coupons had a constant diameter gage length of 1.91 cm (0.75 in.) and a nominal gage diameter of 0.635 cm (0.25 in.). The Ti-6Al-4V and Inconel 718 plates, measuring 17.8 cm x 17.8 cm (7 in. x 7 in.), were cut into straight-sided specimens using the EDM (Electrical Discharge Machining) process. The overall length of the specimens was 17.8 cm (7 in.) and the width was 2.54 cm (1 in.). The Ti-6Al-4V had a nominal thickness of 0.203 cm (0.08 in.), while the Inconel 718 had a nominal thickness of 0.178 cm (0.07 in.). For each material three specimens were tested.

The liquid nitrogen cooled infrared camera of the TSA system employs a 128 x 128 focal plane array of InSb detectors (3 to 5 μm sensitivity). The system operates by recording a periodic temperature change, as viewed by the IR camera, of a specimen subjected to a cyclic mechanical load (see Figure 1). A reference signal from the load cell is used by the software to allow it to monitor only the true thermoelastic change in temperature and to disregard any noise and environmental effects that do not correlate with the reference signal's primary frequency. This is accomplished by using a lock-in detection method (see Reference 8 for an explanation). The lock-in technique filters the thermal response allowing the analysis of only the TSA frequency component that corresponds to the primary frequency of the reference signal. To further improve the TSA signal to noise ratio, the IR signal is monitored, accumulated and averaged over a period of hundreds or thousands of load cycles. When an image is captured, the computer display depicts a dimensionless, digitized value of the average camera signal range corresponding to the cyclic load range for each of the 16384 pixels. For typical structural stress measurements, the dimensionless digital IR values are correlated to a known cyclic stress amplitude (e.g., as measured by a strain gage which represents a finite, local area) and then utilized to map the surface stress amplitudes of the entire structure. Further details concerning the TSA system and the specific settings are given in the Appendix.

Two techniques were utilized to compare the experimental results with the theory. First, direct experimental measurements were conducted for analyzing the mean stress effect. The raw data for these direct measurements were produced in reference 1 and were then modified during this study using newly created temperature correction curves. In addition, the second harmonic of the TSA signal was collected and analyzed.

For convenience the experimental procedure for the direct measurements of the mean stress effect is repeated here. The measurements were accomplished by comparing the camera IR value at various discrete mean stresses while maintaining fixed cyclic stress amplitudes. The test platform employed for inducing the mechanical excitation was a digitally controlled (± 50 kN dynamic / ± 100 kN static) servo-hydraulic test system. The experiments were conducted in load control with a 10-Hertz sinusoidal waveform. Each of the three materials were subjected to a cyclic stress range of 70 MPa (10 ksi). The round TIMETAL 21S specimens had mean stresses varying from –276 MPa (-40 ksi) to 276 MPa (40 ksi). For the straight sided Ti-6Al-4V specimens, the mean stress ranged from 0 to 276 MPa (40 ksi). Finally, the Inconel 718 was subjected to discretely varying mean stresses from 0 to 345 MPa (50 ksi). At least three repetitions were conducted for each individual specimen (except for the TIMETAL 21S, where only one repetition was performed). A test repetition involved stepping through each of the discrete mean stresses and recording an IR signal. The mean stress stepping order was randomized for each test. The camera distance and angle were held constant throughout the experiments. The camera's line of sight was perpendicular to the specimen face, while the distance from the camera lens to the specimen face was maintained at 12.38 cm (4.88 in.). Lastly, it should be noted that all loads were well within the materials' elastic regimes, hence, no plastic deformation occurred.

Next, a comparison was conducted between theory and experiment that concerned the analysis of the second harmonic of the thermoelastic temperature response. Since the TSA system filters all components of the TSA signal except the primary frequency of the reference signal, hardware was developed which allowed the electronics to focus in on the second harmonic of the IR signal. The reference signal from the load cell was passed through a linear frequency doubler (developed for this study and placed in-line with the reference signal) prior to its use by the TSA system, thereby, allowing the TSA system to focus in on the second harmonic. In the earlier studies referred to in the Introduction, a Fast Fourier Transform (FFT) spectrum analyzer was employed for obtaining the amplitude of the TSA signal's second harmonic. This was possible because the IR signal was composed of only a single detector. Here, 16,384 detectors were monitored by the lock-in electronics. To maintain the practicality of the IR array TSA system, the lock-in electronics were utilized during the capture of the second harmonic. An FFT spectrum analyzer was used throughout the study to monitor the purity of the sinusoidal loading function of the servo-hydraulic test system. Furthermore, only the TIMETAL 21S coupons were utilized for the production of the second harmonic TSA data. This is due to the fact that the TIMETAL 21S specimen's geometry allowed for compressive loads. As a result, larger cyclic amplitudes were achieved which assisted in the analysis of the rather small second harmonic TSA signal.

Test preparation included painting all the specimens with an ultra-flat black paint to improve surface emissivity. In addition, K-type thermocouples were spot welded to the back of each specimen (slightly below the gage section) so as to allow temperature monitoring throughout the tests. Since the IR flux is dependent on the source (i.e., specimen) temperature, an empirical equation was used to correct the camera signals to values corresponding to a specimen temperature of 23°C (73.4°F). In reference 1 a single temperature correction curve, acquired from another reference, was utilized for all the TSA data. Here, three empirical relationships were developed corresponding to each of the three material systems. The TIMETAL 21S specimens were cycled at various fixed amplitudes (103 or 207 MPa; 15 or 30 ksi) while maintaining a zero mean stress. For the Ti-6Al-4V and Inconel 718 specimens, the amplitudes were maintained at either 69 or 103 MPa (10 or 15 ksi). The mean stresses for these flat specimens were set equal to the their respective amplitudes so as to avoid any compressive loads. During any particular fixed amplitude test, the absolute specimen temperature was varied between 21 and 27°C (70 and 80°F) while the TSA response was monitored. Heating was achieved by employing a standard hand-held heat gun. Finally, each set of data was normalized by its respective value at 23°C, thereby, allowing the data to reduce to a single line for each material system.

4. RESULTS

Figure 2 displays a typical thermoelastic image as captured by the software. The dimensionless IR camera signal value used throughout this study is an average of an image box in the gage area of the specimen. For the TIMETAL 21S, the box consisted of 300 pixels representing the individual IR detectors (10 wide x 30 long) which were focused on the center portion of the specimen. The boxed area of interest was 0.318 cm x 0.953 cm (0.125 in. x 0.375 in.). For the larger Ti-6Al-4V and Inc 718 specimens, the image box consisted of 3500 detectors (50 x 70), representing a 1.56 cm x 2.15 cm (0.616 in. x 0.846 in.) area.

The values in Table 1 are the linear regression constants for the temperature correction data corresponding to each of the three material systems. Figure 3 displays the data used to produce the linear regression fit for TIMETAL 21S. The temperature correction curve was defined as

$$S_{23^\circ C} = \frac{S}{(q + rT)} \tag{12}$$

where $S_{23^\circ C}$ and S are the corrected and original IR signals, respectively, T is the specimen temperature in degrees Celsius, and q and r are the linear regression constants from Table 1. All IR data presented in this paper are in the temperature corrected form. The relationship of Equation (12) is physically a function of the specimen's IR flux, and assumed to be independent of the subject material. Even so, a cautious approach should be taken on its general use since it is dependent on various experimental factors (e.g., thermocouple location when calibrating TSA response to the monitored temperature). The variations in the regression constants are apparent in Table 1.

In the following paragraphs various normalized mathematical expressions are defined and utilized for both the experimental data as well as for the theoretical formulations. The normalized expressions are required so as to allow a direct comparison between the experimental data, which is in the form of non-dimensional digital values representing the IR camera's electrical

output, and the theoretical formulations, which give a direct value of the temperature range resulting from the thermoelastic effect. The goal here is to verify the experimental behavior with the theory, thereby providing confidence in the experimental measurements. Once confidence is achieved, direct empirical relationships can be developed between the IR camera's digital values and a structure's stress state.

Figure 4 shows the thermoelastic response for the TIMETAL 21S specimens as a function of the mean stress. It is seen that a change in the mean stress from –276 MPa (-40 ksi) to 276 MPa (40 ksi) induced, on average, a 21% increase in the IR signal. Subsequently, the data of the three specimens were pooled and fitted with a linear, first order regression. The constants of the regression fit are presented in Figure 4. The regression constants were used to develop the experimentally determined measure of the mean stress dependence of the thermoelastic parameter (see Equation (10)). This was accomplished by dividing the slope of the regression line by the intercept of the same regression line. Table 2 compares the experimentally measured normalized mean stress effect with the theoretical value obtained using Equation (10) and material properties from reference 9. The comparison indicated a 2.4% difference between the theoretical and experimental values. This result shows a slight improvement over the values obtained in reference 1 where the error between the theory (using the new material properties from reference 9) and experiment (using the old temperature correction curve) was 4.1 %. Also, a comparison was conducted concerning the means of the pooled data at the various discrete cyclic mean stresses. Using the student *t*-test (unpaired) with a 95% confidence level, the smallest statistically significant observable difference in mean stresses for the pooled TIMETAL 21S specimens was calculated as 207 MPa (30 ksi). This result is the same as that obtained in reference 1.

Figures 5 and 6 show the thermoelastic responses for the Ti-6Al-4V and Inconel 718 specimens as functions of the mean stresses. Because no statistically significant differences existed between the specimens at the various discrete mean stresses, the data were pooled for each material type. The regression constants are indicated in the figures. These constants were again used to calculate the normalized mean stress effect as given in Table 2. As a result of using the new temperature correction curves, the errors between the theoretical and experimental values were reduced. The error for the Ti-6Al-4V data is now 35% which compares with a 40% error in reference 1. For the Ti-6Al-4V specimens, an increase of 276 MPa (40 ksi) in the mean stress altered the IR signal by 8%. The smallest statistically significant difference in mean stresses for the pooled Ti-6Al-4V specimens was calculated as 69 MPa (10 ksi). These last two values are equivalent to those given in reference 1.

For the Inconel 718 specimens the error was significantly reduced concerning the mean stress dependence. It should be noted from Figure 6, that there exist two high value outliers at the 0 mean stress, which do not appear to fit the pattern of the data. The increased signals for these points may have been caused by a slight buckling of the relatively thin specimens during the negative load portion of the fully reversed cycle. If the camera were focused on the compressive side of the bend, the IR signal would have an increased value as a consequence of the additive compressive bending stress. As was done in reference 1, the two outlier points were removed from the analysis. Therefore the regression constants shown in Figure 6 were obtained by fitting a linear regression through the reduced data. Using the new regression constants it is seen that the difference between the theoretical and experimental mean stress dependence (Table 2) is 5.5% as compared to 20% in reference 1. An increase of 345 MPa (50 ksi) mean stress resulted in a 4% change in the IR signal. This is equivalent to the reference 1 result. Lastly, a slight improvement was seen when comparing the means at each of the various mean stresses. Here, a 207 MPa (30 ksi) change in mean stress was recognized as being statistically significant as compared to 241 MPa (35 ksi) in reference 1.

Next, the experimental results for the TIMETAL 21S specimens were compared with the theoretical prediction of Equation (8). Presented in Figures 7 and 8 are the first harmonic and second harmonic response curves, respectively. It is seen that the first harmonic is linearly related to the stress amplitude. In keeping with the approach of Wong et al.[7], an equation of the form, $S_\omega = a\,(\Delta\sigma)$ was used to describe the data. A curve fit of the data in Figure (7) yielded a slope of $a = 103.0\ \text{MPa}^{-1}$.

Now focusing on the second harmonic response of Figure (8), it can be seen that the IR response is linearly proportional to the square of the cyclic amplitude and can best be described by an equation of the form, $S_{2\omega} = b\,(\Delta\sigma^2)$. The calculated slope was $b = 6.53 \times 10^{-3}\ \text{MPa}^{-2}$. Next, the ratio of the slopes of the experimentally determined first and second harmonics was calculated as $b/a = 0.634 \times 10^{-4}\ \text{MPa}^{-1}$. This was done so as to allow a comparison with Equation (8). The theoretical ratio, using Equation (8) with a zero mean stress, is as follows:

$$\frac{b}{a} = \left| \frac{1}{4\alpha E^2} \frac{\partial E}{\partial T} \right| \tag{13}$$

Utilizing the TIMETAL 21S material properties in Table 2 (obtained from Castelli et al.[9]), Equation (13) gives a predicted value of $b/a = 0.846 \times 10^{-4}$ MPa^{-1}. The difference between the theoretical and experimental values is 25%. The following section discusses the experimental results.

5. DISCUSSION AND CONCLUSION

The mean stress dependence has been shown for the current material systems, TIMETAL21S, Ti-6Al-4V, and Inconel 718, both experimentally in Figures 4 through 6 as well as theoretically by Equation (10). The errors between the theory and experiment are reasonable and present an improvement over the errors reported in the previous study by the authors (reference 1). The improvements are a result of using temperature correction curves defined during this study. Note that for TIMETAL 21S more accurate material properties were utilized for the theoretical solution. In addition, there was an improvement in the standard deviations of the data in the mean stress dependence curves of Figures 4 through 6.

By utilizing a linear frequency doubler in line with the reference signal, the second harmonic of the IR signal was successfully measured using the TSA system's lock-in electronics. As a result, the practicality of obtaining simultaneous solutions for a 128 x 128 array of IR detectors was maintained. The linear relationship for TIMETAL 21S observed in Figure 7 agrees with the theory where the slope, a, is directly related to the thermoelastic parameter, K. Changing the mean stress would result in a changing slope according to Equation (10). Therefore, it is possible at this point to utilize plots of the first harmonic such as the one in Figure 7 and to use the slopes of such curves to empirically solve for the mean stress. However, a value for the stress amplitude is required. This is only practical when characterizing coupons in a laboratory environment or when testing complex structures which have been fitted with strain gages.

It is seen in Figure 8 that the second harmonic data has a larger spread than the first harmonic data of Figure 7. This is due to the fact that the second harmonic signal is only about 2% of the primary signal. As a result, the second harmonic IR signal is closer to the noise band of the system especially when utilizing small cyclic amplitudes. Also, it is seen that some aberrations in the data did occur. Note that the second harmonic IR values at the 103 MPa (15 ksi) level are, on average, smaller than the IR values at 34 MPa (5 ksi) (see Figure 8). No explanation for this behavior is available, although, it could be due to the low value of the IR signal and its proximity to the noise band of the TSA system. Although the error between the theoretical value of b/a and the experimental b/a is reasonable, improvements can be achieved. The current error is attributed to the sensitivity of the theoretical value to the material properties, and the fact that the material properties utilized here were obtained from reference 9 and not directly measured. Therefore, it appears that confidence was achieved concerning the accuracy of the experimentally obtained data. It is now reasonable to develop empirical equations that directly correlate the TSA results (i.e., the non-dimensional digital values of the IR camera) to the cyclic stress amplitudes and mean stress states of components.

Difficulties do arise with the introduction of multiaxial stresses. The multiaxial problem is very complex, although, some attempts have been made to address the issue of solving for the individual stress components. Past researchers have combined the bulk stress TSA data with numerical methods to obtain stress separation in limited cases. Also, the possibility does exist for combining the results of TSA, which provides information concerning the sum of the principal stresses, and photoelasticity, which provides information on the differences and directions of principal stresses. With on going research in these areas, the TSA method does show promise as a residual stress assessment tool.

APPENDIX

The thermoelastic stress analysis was conducted using the DeltaTherm 1000 system manufactured by Stress Photonics Incorporation. The following system software settings were utilized during IR data acquisition concerning the first and second harmonics of Figures 7 and 8: Accumulation Time = 4.7 seconds; Gain = 1; and AC Channel Integration Time constant = 120 seconds. Collection time for any given test condition was 240 seconds. This consisted of 120 seconds to collect the first harmonic and then activating the frequency doubler and obtaining a 120 seconds reading for the second harmonic. Note the timer was reset after each 120 second capture. Lastly, the data which was obtained from reference 1 had an Accumulation Time = 4.7; Gain=2; and an AC Channel Integration Time constant = 300 seconds (see Figures 4 through 6).

REFERENCES

1. A.L. Gyekenyesi and G.Y. Baaklini, "Thermoelastic Stress Analysis: The Mean Stress Effect in Metallic Alloys," *Proceedings of SPIE Conference on the NDE of Aging Materials and Composites*, Newport Beach, CA, March 1–4, 1999.
2. J.R. Lesniak, and B.R. Boyce, "A High-Speed Differential Thermographic Camera," *SEM Spring Conference Proceedings*, Baltimore, Maryland, June 6–8, 1994, pp. 491–497.
3. W. Thomson (Lord Kelvin), "On the Dynamical Theory of Heat," *Trans. Roy. Soc. Edinburgh*, Volume 20, 1853, pp. 261–283.
4. A.S. Machin, J.G. Sparrow, and M.G. Stimson, "Mean Stress Dependence of the Thermoelastic Constant," *Strain*, Volume 23, 1987, pp. 27–30.
5. S.A. Dunn, D. Lombardo, and J.G. Sparrow, "The Mean Stress Effect in Metallic Alloys and Composites," *SPIE Stress and Vibration: Recent Developments in Industrial Measurement and Analysis*, Volume 1084, 1989, pp. 129–142.
6. A.K. Wong, R. Jones, and J.G. Sparrow, "Thermoelastic Constant or Thermoelastic Parameter?" *J. Phys. Chem. Solids*, Volume 48, 1987, pp. 749–753.
7. A.K. Wong, J.G. Sparrow, and S.A. Dunn, "On the Revised Theory of the Thermoelastic Effect," *J. Phys. Chem. Solids*, Volume 49, 1988, pp. 395–400.
8. J.R. Lesniak and B.R. Boyce, "Differential Thermography Applied to Structural Integrity Assessment," *Proceedings of the International Conference on Thermal Sensing and Imaging Diagnostic Applications*, Orlando, Florida, April 19–21, 1995, Vol. 2473, pp. 179–189.
9. M.G. Castelli, S.M. Arnold, and A.F. Saleeb, "Specialized Deformation Tests for the Characterization of a Viscoplastic Model: Application to a Titanium Alloy," NASA TM–106268, in print.
10. M.G. Castelli, B.A. Lerch, and D.J. Keller, "A Comparison of Deformation Behaviors of HIPed Foil and Sheet Titanium Alloys," HITEMP Review 1999: Advanced High Temperature Engine Materials Technology Project, NASA CP–208915, Vol. 2, 1999.
11. "Metals Handbook: Desk Edition," 9th ed., H.E. Boyer and T.L. Gall, eds., American Society for Metals, 1997.
12. "High Temperature, High Strength Nickel Base Alloys," Inco Limited, New York, NY, 1977.

TABLE 1. LINEAR REGRESSION CONSTANTS FOR TEMPERATURE CORRECTION CURVES.

Material	Intercept, Norm TSA Signal* (q: Eq. 12)	Slope, (Norm TSA)/(Temp. °C) (r: Eq. 12)
TIMETAL 21S	0.337	0.0288
Ti-6Al-4V	0.0236	0.0425
Inconel 718	-0.0479	0.0455

*TSA signals normalized by respective TSA value at 23°C (see Figure 3).

TABLE 2. COMPARISON OF THEORETICAL AND EXPERIMENTAL MEAN STRESS DEPENDENCE OF K.

Material*	α, 10^{-6}/°K	$E_{23°C}$, GPa	$\partial E/\partial T$ MPa/°K	Theory Eq. (10) MPa^{-1}	Experiments MPa^{-1}
TIMETAL 21S	8.24	116	-37.6	3.39×10^{-4}	3.47×10^{-4}
Ti-6Al-4V	9.06	120	-61.8	4.75×10^{-4}	3.07×10^{-4}
Inconel 718	12.2	205	-57.7	1.12×10^{-4}	1.18×10^{-4}

*Material properties obtained from references 9 through 12.

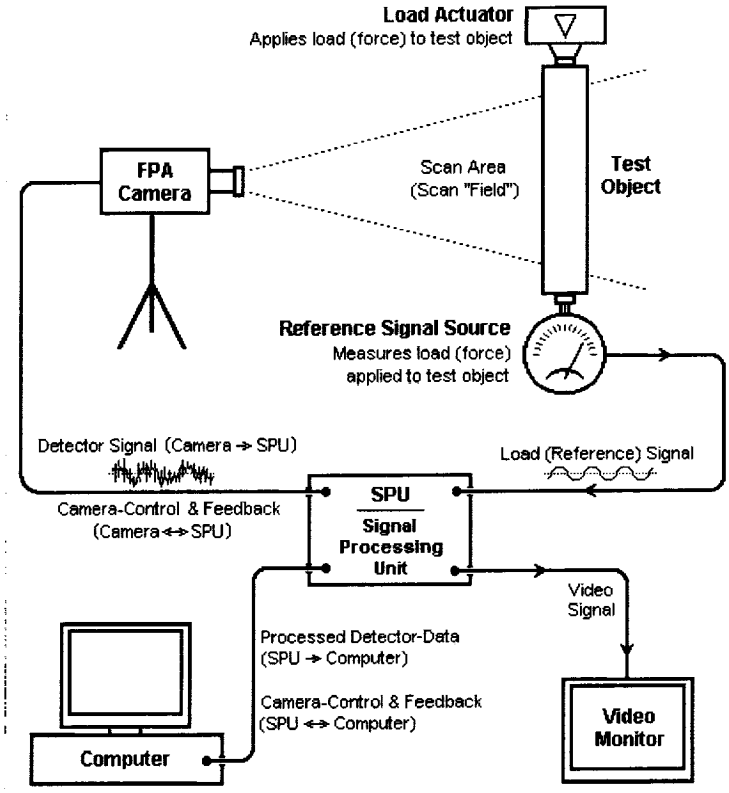

Figure 1 Schematic diagram of TSA system (DeltaTherm 1000 User's Manual).

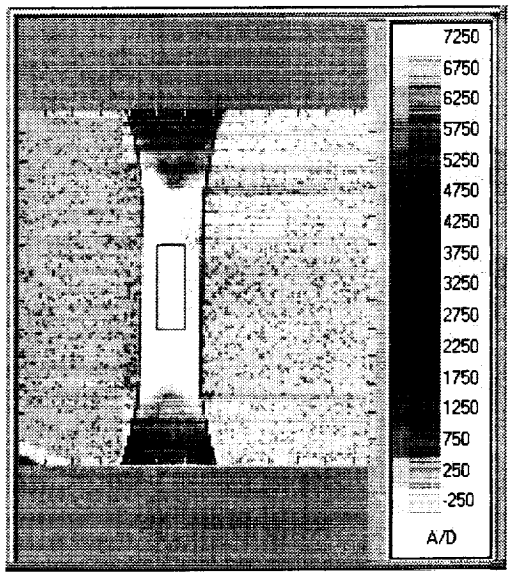

Figure 2 Typical IR test image for a TIMETAL 21S specimen. The rectangular box within the specimen indicates the area where the average signal was obtained. The scale displays the dimensionless digital values of the IR camera signal.

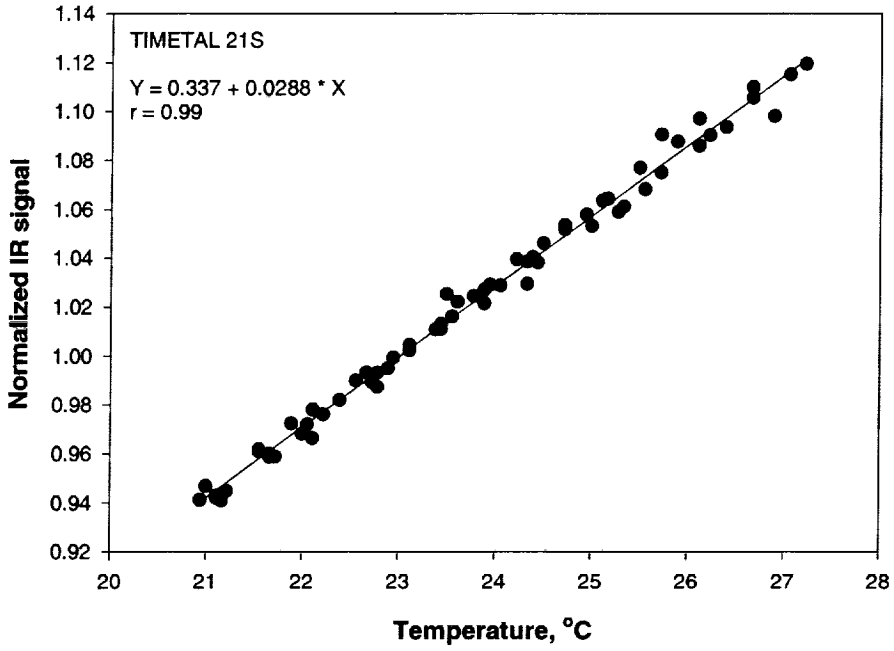

Figure 3 Temperature dependence of IR signal for TIMETAL 21S specimens. Data consists of eight tests utilizing three specimens. All tests normalized by corresponding IR signals at 23°C. Equation represents first order linear regression fit of all data.

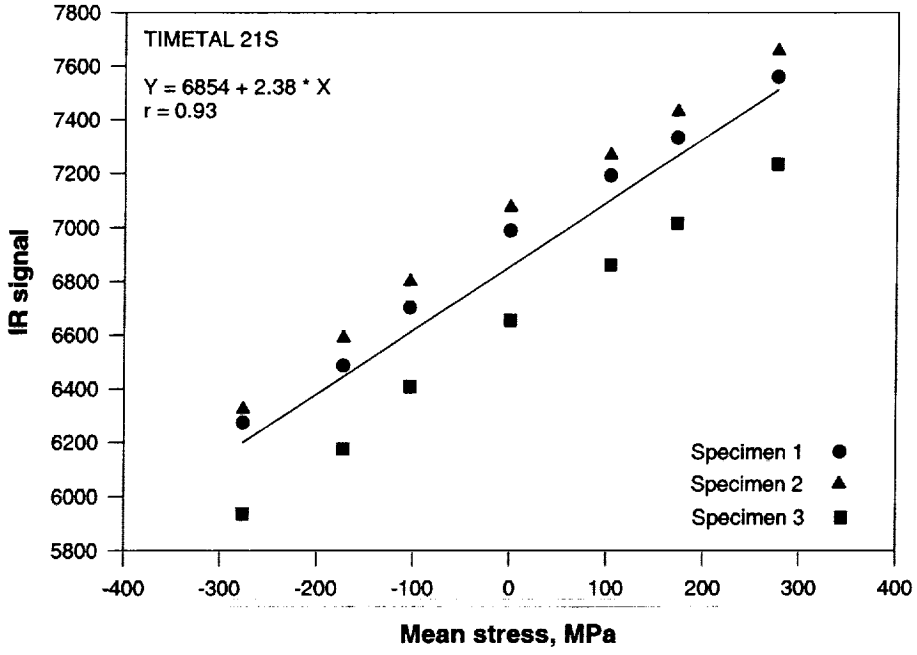

Figure 4 Mean stress dependence of IR signal for TIMETAL 21S utilizing three specimens. (σ_{amp} = 34 MPa (5 ksi)). Equation represents first order linear regression fit of all data.

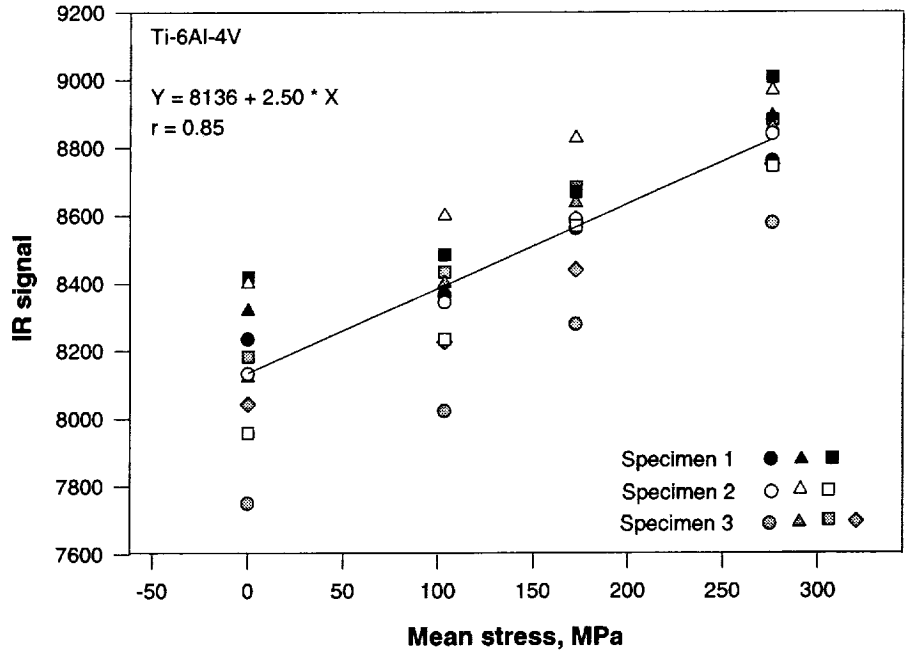

Figure 5 Mean stress dependence of IR signal for Ti-6Al-4V utilizing three specimens and three repetitions each (σ_{amp} = 34 MPa (5 ksi)). Equation represents first order linear regression fit of all data.

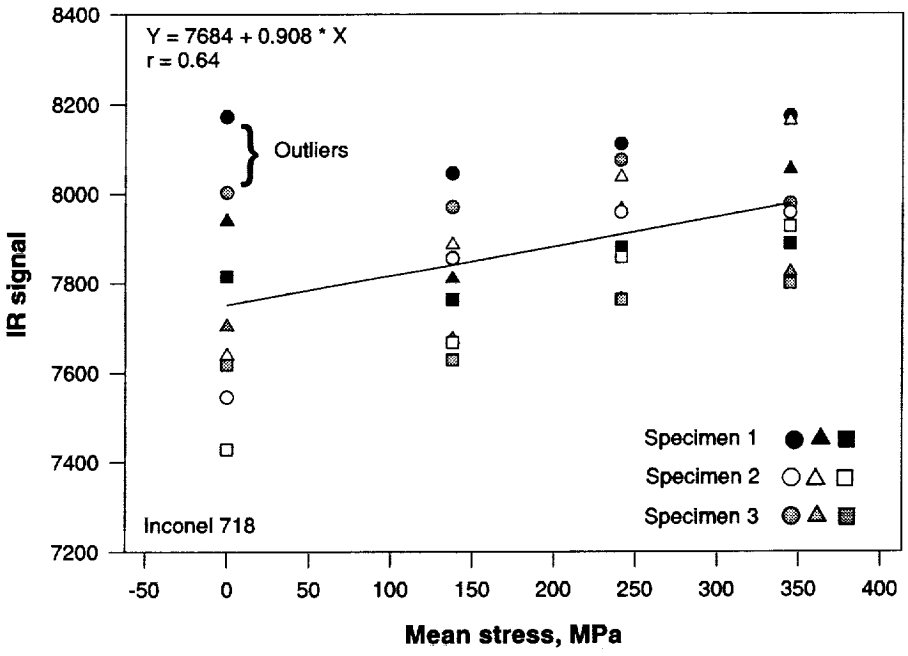

Figure 6 Mean stress dependence of IR signal for Inconel 718 utilizing three specimens with three repetitions each (σ_{amp} = 34 MPa (5 ksi)). Equation represents first order linear regression fit of data excluding outliers.

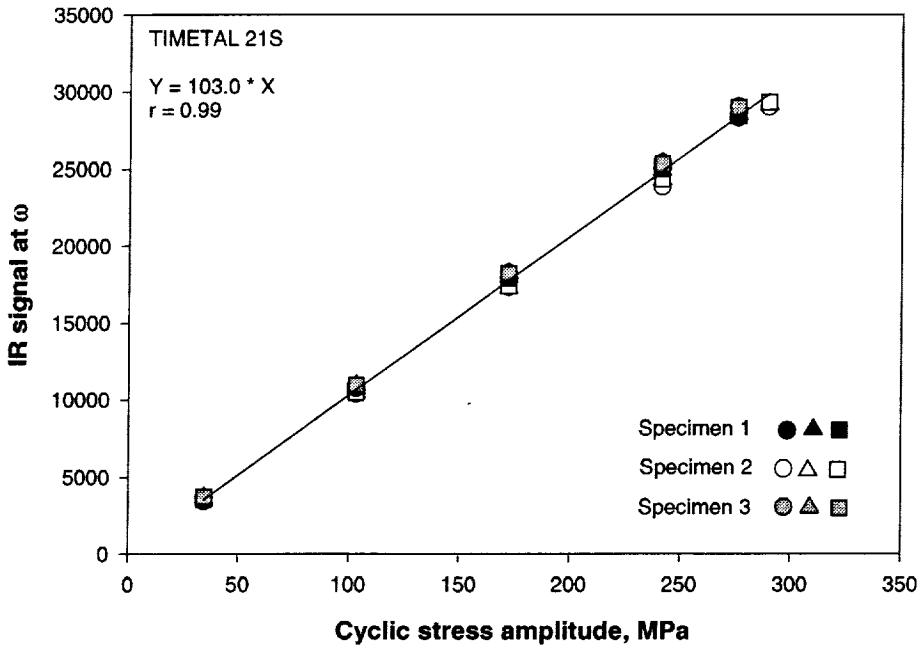

Figure 7 First harmonic IR signal output at various stress amplitudes ($\sigma_m = 0$) for TIMETAL 21S specimens. The plot contains data from three specimens; each with three repetitions. Equation represents first order linear regression fit of all data.

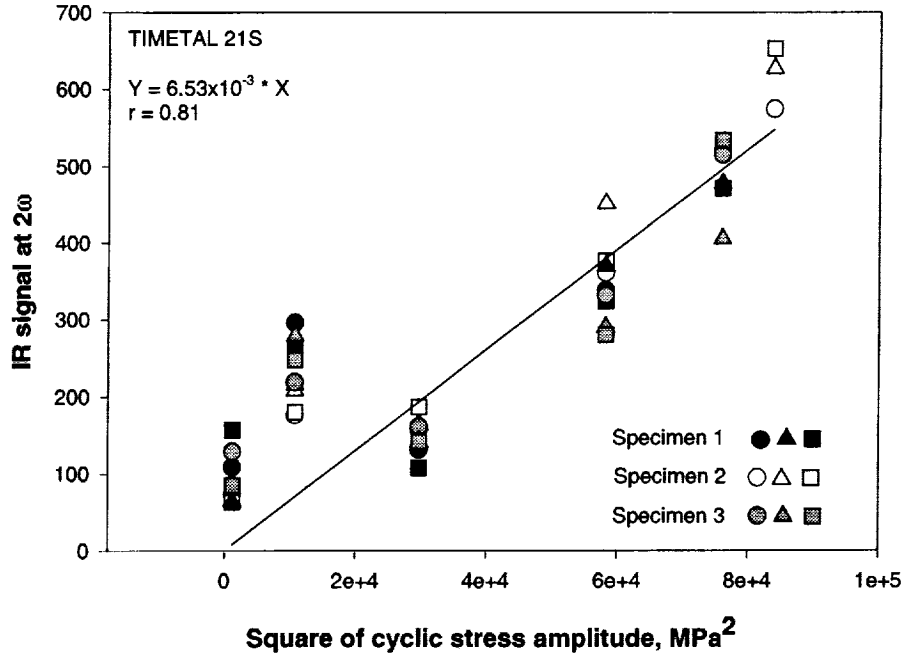

Figure 8 Second harmonic IR signal output at various stress amplitudes ($\sigma_m = 0$) for TIMETAL 21S specimens. The plot contains data from three specimens; each with three repetitions. Equation represents first order linear regression fit of all data.

REPORT DOCUMENTATION PAGE

Form Approved
OMB No. 0704-0188

1. AGENCY USE ONLY (*Leave blank*)	2. REPORT DATE	3. REPORT TYPE AND DATES COVERED
	February 2001	Technical Memorandum

4. TITLE AND SUBTITLE

Quantifying Residual Stresses by Means of Thermoelastic Stress Analysis

5. FUNDING NUMBERS

WU–728–30–20–00

6. AUTHOR(S)

Andrew L. Gyekenyesi and George Y. Baaklini

7. PERFORMING ORGANIZATION NAME(S) AND ADDRESS(ES)

National Aeronautics and Space Administration
John H. Glenn Research Center at Lewis Field
Cleveland, Ohio 44135–3191

8. PERFORMING ORGANIZATION REPORT NUMBER

E–12628

9. SPONSORING/MONITORING AGENCY NAME(S) AND ADDRESS(ES)

National Aeronautics and Space Administration
Washington, DC 20546–0001

10. SPONSORING/MONITORING AGENCY REPORT NUMBER

NASA TM—2001-210697

11. SUPPLEMENTARY NOTES

Prepared for the Nondestructive Evaluation of Aging Materials and Composites IV sponsored by the Society of Photo-Optical Instrumentation Engineers, Newport Beach, California, March 8–9, 2000. Andrew L. Gyekenyesi, Ohio Aerospace Institute, 2001 Aerospace Parkway, Brook Park, Ohio 44142 (work funded by NASA Grant NAG3–755); and George Y. Baaklini, NASA Glenn Research Center. Responsible person, George Y. Baaklini, organization code 5920, 216–433–6016.

12a. DISTRIBUTION/AVAILABILITY STATEMENT

Unclassified - Unlimited
Subject Category: 39 Distribution: Nonstandard

Available electronically at http://gltrs.grc.nasa.gov/GLTRS

This publication is available from the NASA Center for AeroSpace Information, 301–621–0390.

12b. DISTRIBUTION CODE

13. ABSTRACT ***(Maximum 200 words)***

This study focused on the application of the Thermoelastic Stress Analysis (TSA) technique as a tool for assessing the residual stress state of structures. TSA is based on the fact that materials experience small temperature changes when compressed or expanded. When a structure is cyclically loaded, a surface temperature profile results which correlates to the surface stresses. The cyclic surface temperature is measured with an infrared camera. Traditionally, the amplitude of a TSA signal was theoretically defined to be linearly dependent on the cyclic stress amplitude. Recent studies have established that the temperature response is also dependent on the cyclic mean stress (i.e., the static stress state of the structure). In a previous study by the authors, it was shown that mean stresses significantly influenced the TSA results for titanium- and nickel-based alloys. This study continued the effort of accurate direct measurements of the mean stress effect by implementing various experimental modifications. In addition, a more in-depth analysis was conducted which involved analyzing the second harmonic of the temperature response. By obtaining the amplitudes of the first and second harmonics, the stress amplitude and the mean stress at a given point on a structure subjected to a cyclic load can be simultaneously obtained. The experimental results showed good agreement with the theoretical predictions for both the first and second harmonics of the temperature response. As a result, confidence was achieved concerning the ability to simultaneously obtain values for the static stress state as well as the cyclic stress amplitude of structures subjected to cyclic loads using the TSA technique. With continued research, it is now feasible to establish a protocol that would enable the monitoring of residual stresses in structures utilizing TSA.

14. SUBJECT TERMS

Thermoelastic stress analysis; Residual stress; Mean stress; SPATE; Thermoelastic constant; TSA

15. NUMBER OF PAGES

18

16. PRICE CODE

A03

17. SECURITY CLASSIFICATION OF REPORT	18. SECURITY CLASSIFICATION OF THIS PAGE	19. SECURITY CLASSIFICATION OF ABSTRACT	20. LIMITATION OF ABSTRACT
Unclassified	Unclassified	Unclassified	